

Steady Sailing Performance of a Ship in the Proximity to the Bank under Windy Conditions

Hironori Yasukawa (Hiroshima University)¹

ABSTRACT

This paper presents a method to efficiently calculate steady sailing conditions such as check helm, speed drop, hull drift angle etc. of a ship moving in parallel to a bank wall under steady wind, together with the course stability at the equilibrium condition. Using this method, this study investigates the bank effect on the steady sailing condition and the course stability of a pure car carrier in steady wind and it evaluates the limiting wind condition for safe navigation (maneuvering limit). In case of head wind, a significant speed drop appears. In case of oblique head wind from the port side, the hull drift angle increases significantly and there is a distinct possibility that the ship touches the bank wall. In case of oblique following wind from the port side, the check helm increases significantly because the wind force is added to the bank suction force. This becomes critical when the ship moves closer to the bank and in more shallow water areas, and the maneuvering limit level becomes more severe. The present method is a useful tool for measuring the maneuvering limit of a ship moving in close proximity to the bank under steady wind.

Key words

Bank effect; Steady sailing condition; Course stability; MMG-model; Pure car carrier

¹corresponding author: Department of transportation and environmental systems, Hiroshima University, Kagamiyama 1-4-1, Higashi-Hiroshima, 739-8527, Hiroshima, Japan, email: yasukawa@hiroshima-u.ac.jp

List of symbols

Abbreviation

CS	Course stability
MCR	Maximum Continuous Rating (of main engine)
MMG	Maneuvering Modeling Group
NOR	NOrmal Rating
PCC	Pure Car Carrier
SSC	Steady Sailing Condition

Greek symbols

α_z	Vertical acting point of the lateral added mass component m_y
β	Hull drift angle at midship
$\overline{\gamma_R}$	Averaged flow straightening coefficient
δ	Rudder angle
η	Lateral deviation of the ship centerline at midship position from x_0 -axis
θ_A	Relative wind direction
θ_W	Absolute wind direction
ρ	Water density
ρ_a	Air density
ϕ	Roll angle
ψ	Ship heading
∇	Displacement volume of the ship

Roman symbols

A_X, A_Y	Front and side profile areas of the ship in air, respectively
A_R	Rudder profile area
a_H	Rudder force increase factor
B	Ship breadth
C_b	Block coefficient
$C_{XA}, C_{YA}, C_{NA}, C_{KA}$	Aerodynamic force coefficients with respect to surge force, lateral force, yaw moment and roll moment, respectively
D_P	Propeller diameter
d	Ship draft
F_N	Rudder normal force
\overline{GM}	Metacentric height
G_1, G_2	Control gains for autopilot
g	Gravity acceleration
H_R	Rudder span length
h	Water depth
I_{xx}, I_{zz}	Moment of inertia of the ship around x - and z -axes, respectively
J_{xx}, J_{zz}	Added moment of inertia around x - and z -axes, respectively
\overline{KM}	Metacenter height above baseline
$K_{\dot{\phi}}, K_{\dot{\phi}\dot{\phi}}$	Roll damping coefficients

k_{xx}	Radius of roll gyration including added moment of inertia with respect to the roll
L	Ship length between perpendiculars
m	Ship's mass
m_x, m_y	Added masses of the x -axis direction and y -axis direction, respectively
N_{MCR}	Propeller revolution at MCR
N_P	Propeller revolution
N_S	Propeller revolution at P_S
$N'_v, N'_r, N'_\phi, N'_{vvv}$ etc.	Hydrodynamic derivatives with respect to yaw moment
$o - xyz$	Horizontal body fixed coordinate system considering the origin at midship
$o_0 - x_0 y_0 z_0$	Space fixed coordinate system
P_{MCR}	Engine power at MCR
P_S	Engine power at NOR with 15% sea margin
Q_{EMAX}	Maximum propeller torque of the main engines
R_0	Ship resistance in straight moving
r	Yaw rate
s	Distance from the bank toe to ship side
T	Propeller thrust
t	Time
t_P	Thrust deduction factor
t_R	Steering resistance deduction factor
U	Resultant speed $(= \sqrt{u^2 + v_m^2})$
U_W	Absolute wind velocity
u, v	Surge velocity and lateral velocity at the center of gravity, respectively
V_A	Relative wind velocity
V_S	Design speed of the ship
v_m	Lateral velocity at midship
W	Distance from the bank toe at the sea bottom to ship center line
X, Y, N, K	Surge force, lateral force, yaw moment, and roll moment with the exception of added mass components, respectively
X_A, Y_A, N_A, K_A	Surge force, lateral force, yaw moment, and roll moment due to wind
X_H, Y_H, N_H	Surge force, lateral force, and yaw moment acting on the ship hull with the exception of added mass components, respectively
X_P	Surge force due to the propeller
X_R, Y_R, N_R	Surge force, lateral force, and yaw moment by steering, respectively
$X'_{vv}, X'_{rr}, X'_{\phi\phi}, X'_{vrv}$ etc.	Hydrodynamic derivatives with respect to surge force
x_G	Longitudinal coordinate of the center of gravity of the ship
x_H	Longitudinal coordinate of the acting point of the additional lateral force component induced by steering
x_R	Longitudinal coordinate of the rudder position $(=-0.5L)$
Y_{H0}	Hull lateral force excluding bank effect
$Y_{H\eta}$	Hull lateral force components including bank effect
$Y'_v, Y'_r, Y'_\phi, Y'_{vvv}$ etc.	Hydrodynamic derivatives with respect to lateral force

z_G	Vertical coordinate of the center of gravity of the ship
z_H	Vertical coordinate of the acting point of the hull lateral force
z_{H0}	Vertical coordinate of the acting point of hull lateral force components excluding bank effect
$z_{H\eta}$	Vertical coordinate of the acting point of hull lateral force components including bank effect
z_R	Vertical coordinate of the acting point of the rudder force
subscript 0	implies a steady term
substituting Δ	implies an unsteady term

1 Introduction

As ship size increases, a cascading effect occurs that forces ships to sometimes sail close to banks in ports and channels. To investigate the navigation safety of ships in such restricted water areas, we have to capture their hydrodynamic force characteristics (the hydrodynamic forces acting on the hull in obliquely moving and/or turning, and the respective rudder force) using captive model tests. Consequently, and based on the force characteristics, we have to evaluate parameters such as the rudder deflection (check helm) and hull drift angle to facilitate safe navigation and course stability. However, these studies should be performed, not only in environments of calm water but also in environments characterized by significant external disturbances such as strong winds. Nonetheless, and in addition to assessing water depth and the distance between bank and ship in the tank tests, it is equally necessary to change several parameters including hull drift angle, rudder angle, and yaw rate to capture the hydrodynamic force characteristics of the ship in such restricted water areas. Therefore, the mere use of tank tests will not provide an efficient evaluation of the hydrodynamic force characteristics. In fact, current literature typically fails to consider these series of data when investigating the ship's check helm and course stability.

Fujino [1][2] used tank tests to measure the hydrodynamic forces acting on a ship moving in a channel with changing parameters such as water depth, distance from the ship to the centerline of the channel, hull drift angle, rudder angle, and so on. Consequently, and based on their results, the authors calculated the necessary check helm and hull drift angle required to overcome the bank suction force. Moreover, this study provided a theoretical framework to investigate the ship's course stability moving in the centerline of the channel.

Eda [3] performed a similar study and presented distinct guidelines that indicate the acceptable ship size relative to the respective waterway dimensions.

On the other hand, Sano et al. [4] derived a course stability criterion for a ship's off-centerline in a channel. More specifically, the authors investigated the course stability for an inland container ship based on its measured hydrodynamic force derivatives moving in a channel with variation of the parameters mentioned above.

Furthermore, Yasukawa[5] presented an analytic method to evaluate a ship's course stability in proximity to a bank. To evaluate its hydrodynamic derivatives, oblique towing tests (OTT) were performed to register the bank effect on these derivatives in both deep and shallow waters. In addition, captive model tests were performed by varying the heel angles. This could, in turn, allow the authors to further comprehend and evaluate the influence of the heel effect on the derivatives. Consequently, and using the derivatives obtained, the course stability was analyzed for a pure car carrier in proximity to the bank. However, all these studies were solely conducted under calm water conditions.

External-disturbance effects such as winds and waves cannot be ignored when discussing the actual maneuvering limit. In particular, the effect of the wind in restricted water areas such as ports is very essential. For instance, Yasukawa et al.[6] investigated the equilibrium condition (check helm, hull drift angle, etc.) required for safe course-keeping while at the same time evaluating the ship's course stability in a channel under steady wind by extending the method initially presented by Sano et al.[4]. In this study, however, the ship was assumed to be travelling at a constant speed, a prerequisite that was facilitated by inducing appropriate adjustments to the main engine. Thus, there are

a few comprehensive studies that have investigated ships' navigation safety close to the bank under windy conditions.

In this study, an analysis result is presented and which pertains to steady sailing conditions (SSC) such as check helm, hull drift angle, speed drop, etc. Furthermore, this study intends to evaluate the course stability (CS) of a pure car carrier (PCC) in proximity to the bank under steady wind without performing any approximations with respect to the ship speed. A calculation method of the SSC and the CS of ships in open sea under external disturbances due to wind and waves[7] is extended to safeguard ships in close proximity to the bank and under windy conditions. It should be mentioned that the experimental data presented in an earlier study [5] are used in our paper because the ship's hydrodynamic force characteristics in proximity to the bank are required for our calculations. Finally, and based on the analysis results of the variation of wind speed, wind direction, distance between ship and bank, water depth etc., the limiting wind condition (maneuvering limit) for safe navigation is discussed.

2 Base Equations for Steady Sailing Performance of a Ship Close to a Bank in Wind

2.1 Coordinate systems

Fig.1 demonstrates the coordinate systems and notations used in this paper. Consider a ship moving in close proximity to a bank. The ship moves in a straight line along the bank wall. The bank horizontal shape is considered to be uniform, and the bank is at the starboard side of the ship. The bank wall is inclined by 45° as shown in Fig.1 (left). Water depth is denoted by h and is assumed to be constant.

Consider the space-fixed coordinate system $o_0 - x_0 y_0 z_0$ where the $x_0 - y_0$ plane coincides with the still water surface and the z_0 -axis is taken vertically downwards. Furthermore, the x_0 -axis is taken in parallel to the bank wall with a distance W from the bank toe at the sea bottom as shown in Fig.1. s is the distance from the bank toe to ship side. The y_0 -axis is taken laterally according to the right-handed system. The ship is assumed to sail only in the region defined by $y_0 \geq 0$. When the ship sails in the region defined by $y_0 < 0$, then the bank effect vanishes.

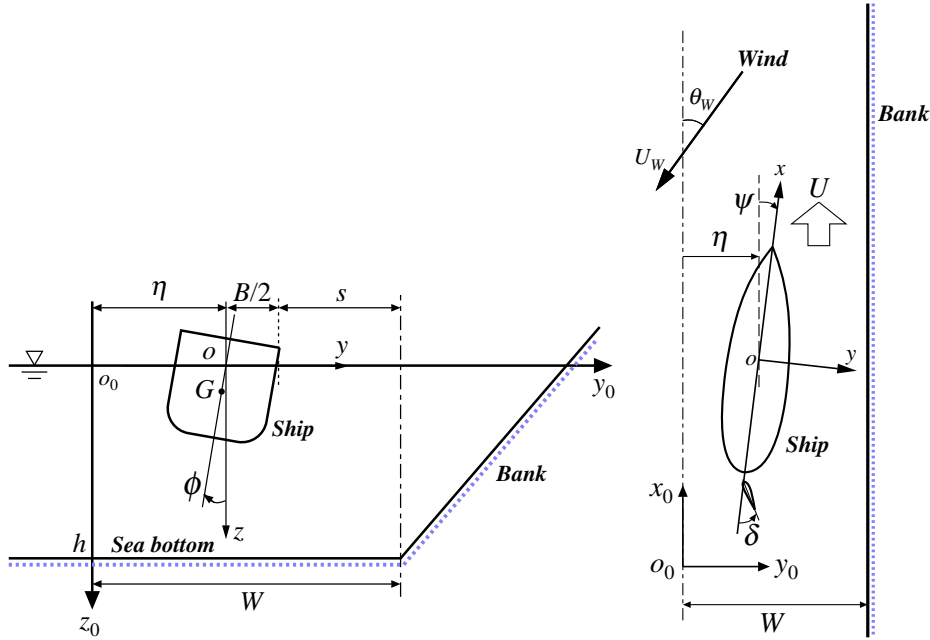


Fig. 1: Coordinate systems and notations (left: vertical ship section view, right: horizontal plane view)

In addition, consider the horizontal body-fixed coordinate system[8] $o - xyz$. The x -axis is taken towards the ship's bow direction, whereas the y -axis is taken laterally and the z -axis is taken vertically downwards. Furthermore, the $x - y$ plane coincides with the still water surface. Therefore, the origin o is located at the position of the midship on the still water surface. The heading angle ψ is defined as the direction between x_0 -axis and x -axis, whereas the roll angle is denoted by ϕ . The clockwise rotation is positive for roll when looking from the ship's stern towards the fore direction. u and v denote the

velocity components of x -axis and y -axis respectively, and r is the yaw rate around the z -axis. Furthermore, δ denotes the rudder angle. The center of gravity G is approximately located at $(x_G, 0, z_G)$. Among z_G , \overline{GM} and \overline{KM} , the following relation applies:

$$z_G \simeq \overline{GM} - \overline{KM} + d \quad (1)$$

where \overline{KM} is metacenter height from ship bottom, \overline{GM} is the metacentric height and d is ship draft. Then, lateral velocity component at midship position v_m is expressed as:

$$v_m = v - x_G r + z_G \dot{\phi} \quad (2)$$

In this equation, the dot notation implies the ordinary differential with respect to time t . Total velocity U is defined as:

$$U = \sqrt{u^2 + v_m^2} \quad (3)$$

and the hull drift angle at midship position β is evaluated by

$$\beta = \tan^{-1}(-v_m/u) \quad (4)$$

Note that ψ coincides with β when the ship moves towards the direction of x_0 -axis as shown in Fig.1. Lateral deviation of the ship centerline at midship position from x_0 -axis is denoted by η . Between η and the velocity components, u and v_m , the following relation is hold as

$$\dot{\eta} = u \sin \psi + v_m \cos \psi \quad (5)$$

The absolute wind velocity is denoted as U_W , and the absolute wind direction is denoted by θ_W as shown in Fig.1. In case of $\psi = 0^\circ$, the range of $0^\circ \sim 180^\circ$ in θ_W suggests that the wind blows on the ship from the starboard side, and the range of $-180^\circ \sim 0^\circ$ in θ_W suggests that the wind blows on the ship from the port side.

2.2 Motion equations

In the horizontal body-fixed coordinate system, the motion equations for a ship's surge, sway, yaw, and roll are expressed as[9]:

$$\left. \begin{aligned} (m + m_x)\dot{u} - (m + m_y)v_m r - m x_G r^2 + m z_G r \dot{\phi} &= X \\ (m + m_y)\dot{v}_m + (m + m_x)ur + m x_G \dot{r} - (m_y \alpha_z + m z_G)\ddot{\phi} &= Y \\ (I_{zz} + J_{zz} + m x_G^2)\dot{r} + m x_G(\dot{v}_m - z_G \ddot{\phi} + ur) &= N \\ (I_{xx} + J_{xx} + m z_G^2)\ddot{\phi} - (m_y \alpha_z + m z_G)\dot{v}_m - m z_G(x_G \dot{r} + ur) &= K \end{aligned} \right\} \quad (6)$$

Here, m is the ship's mass, and I_{xx} and I_{zz} are the moment of inertias for roll and yaw, respectively. Moreover, m_x , m_y , J_{zz} and J_{xx} denote the added mass for surge, the added mass for sway, the added moment of inertia for yaw, and the added moment of inertia for roll, respectively. These parameters change with lateral deviation from x_0 -axis η . α_z is the vertical acting point of the lateral added mass component m_y . X is the surge force excluding the added mass component, Y is the lateral force excluding the added mass component, N is the yaw moment around midship excluding the added moment of inertia

component, and K is the roll moment around the x -axis excluding the added moment of inertia component. The unknown variables in the motion equations are the longitudinal velocity component u , the lateral velocity component v_m , the yaw rate r and the roll angle ϕ . Consequently, the next step is to solve these motion equations.

X , Y and N are expressed as:

$$\left. \begin{aligned} X &= X_H + X_R + X_P + X_A \\ Y &= Y_H + Y_R + Y_A \\ N &= N_H + N_R + N_A \end{aligned} \right\} \quad (7)$$

Subscript H , R , P and A in the right-hand side of Eq.(7) mean hull, rudder and propeller and aerodynamic forces (wind forces), respectively. The detailed explanations of propeller force (X_P), rudder forces (X_R , Y_R , N_R) and aerodynamic forces (X_A , Y_A , N_A) are not taken into consideration at present. However, these parameters have already been defined and described in Ref.[7][10]. Hence, in this paper we assume that the bank effect appears only in the hydrodynamic forces acting on ship hull.

2.3 Hull hydrodynamic forces

Hydrodynamic forces acting on ship hull (X_H , Y_H , N_H) are expressed as:

$$\left. \begin{aligned} X_H &= (1/2)\rho L d U^2 X'_H(v'_m, r', \phi, \eta') \\ Y_H &= (1/2)\rho L d U^2 Y'_H(v'_m, r', \phi, \eta') \\ N_H &= (1/2)\rho L^2 d U^2 N'_H(v'_m, r', \phi, \eta') \end{aligned} \right\} \quad (8)$$

where ρ , L and d are water density, ship length and ship draft, respectively. v'_m is defined by v_m/U , r' is defined by rL/U and η' is defined by η/L . Here, X'_H , Y'_H and N'_H are expressed as:

$$\begin{aligned} X'_H(v'_m, r', \phi, \eta') &= -R'_0 + X'_{vv}v_m'^2 + X'_{vr}v'_m r' + X'_{rr}r'^2 + X'_{vvv}v_m'^4 \\ &\quad + X'_{v\phi}v'_m \phi + X'_{r\phi}r' \phi + X'_{\phi\phi}\phi^2 + X'_{\eta\eta}\eta'^2 + X'_{v\eta}v'_m \eta' \end{aligned} \quad (9)$$

Here, R'_0 is the resistance coefficient in straight moving, and X'_{vv} , X'_{vr} , X'_{rr} etc. are defined as the hydrodynamic derivatives on maneuvering. X'_H is expressed as the sum of R'_0 , and it is the 2nd-order polynomial function of v'_m , r' , ϕ and η' except from the X'_{vvv} -term.

Y'_H and N'_H are expressed as 1st and 3rd-order polynomial function of v'_m , r' , ϕ and η' .

$$Y'_H(v'_m, r', \phi, \eta') = Y'_{H0}(v'_m, r', \phi) + Y'_{H\eta}(v'_m, \eta') \quad (10)$$

$$\begin{aligned} Y'_{H0}(v'_m, r', \phi) &= Y'_v v'_m + Y'_r r' + Y'_{vv}v_m'^3 + Y'_{vr}v_m'^2 r' + Y'_{vrr}v'_m r'^2 + Y'_{rrr}r'^3 \\ &\quad + Y'_\phi \phi + Y'_{v\phi}v_m'^2 \phi + Y'_{v\phi\phi}v'_m \phi^2 + Y'_{rr\phi}r'^2 \phi + Y'_{r\phi\phi}r' \phi^2 \end{aligned} \quad (11)$$

$$Y'_{H\eta}(v'_m, \eta') = Y'_\eta \eta' + Y'_{\eta\eta}\eta'^3 + Y'_{v\eta}v_m'^2 \eta' + Y'_{v\eta\eta}v'_m \eta'^2 \quad (12)$$

$$N'_H(v'_m, r', \phi, \eta') = N'_{H0}(v'_m, r', \phi) + N'_{H\eta}(v'_m, \eta') \quad (13)$$

$$\begin{aligned} N'_{H0}(v'_m, r', \phi) &= N'_v v'_m + N'_r r' + N'_{vv}v_m'^3 + N'_{vr}v_m'^2 r' + N'_{vrr}v'_m r'^2 + N'_{rrr}r'^3 \\ &\quad + N'_\phi \phi + N'_{v\phi}v_m'^2 \phi + N'_{v\phi\phi}v'_m \phi^2 + N'_{rr\phi}r'^2 \phi + N'_{r\phi\phi}r' \phi^2 \end{aligned} \quad (14)$$

$$N'_{H\eta}(v'_m, \eta') = N'_\eta \eta' + N'_{\eta\eta}\eta'^3 + N'_{v\eta}v_m'^2 \eta' + N'_{v\eta\eta}v'_m \eta'^2 \quad (15)$$

In the equations mentioned above, η' -terms are included so as to consider the bank effect. If we delete all the η' -terms, the remaining equations will then represent open sea (no bank) conditions as indicated in Ref.[7].

Roll moment K is expressed as:

$$K = -Y_{H0}z_{H0} - Y_{H\eta}z_{H\eta} - Y_R z_R - mg\overline{GM}\phi + K_{\dot{\phi}}\dot{\phi} + K_{\dot{\phi}\dot{\phi}}\dot{\phi}|\dot{\phi}| + K_A \quad (16)$$

On the right hand side of Eq.(16), the first term refers to the roll moment acting on the hull, except from the bank effect, the second term refers to the roll moment acting on the hull due to the bank suction force, and the third term refers to the roll moment due to steering. Furthermore, they can all be expressed by multiplying the lateral force components (Y_{H0} , $Y_{H\eta}$, Y_R) by their vertical acting points (z_{H0} , $z_{H\eta}$, z_R). In addition, the fourth term refers to the roll restoring moment, whereas the fifth and the sixth terms refer to the roll damping moment. $K_{\dot{\phi}}$ and $K_{\dot{\phi}\dot{\phi}}$ are roll damping coefficients. Finally, the seventh term refers to the roll moment as a result of the respective wind.

2.4 Equations for steady sailing performance

Consider the ship's behavior following small disturbances on the ship's moving in parallel to a bank wall under steady wind. Here, we express the variables in the motion equations, u , v_m , ψ , ϕ , δ and η , as the sum of the static (steady term) and variation components (unsteady term):

$$\left. \begin{aligned} u &= u_0 \\ v_m &= v_0 + \Delta v \\ \psi &= \psi_0 + \Delta\psi \\ \phi &= \phi_0 + \Delta\phi \\ \delta &= \delta_0 + \Delta\delta \\ \eta &= \eta_0 + \Delta\eta \end{aligned} \right\} \quad (17)$$

In Eq.(17), subscript 0 indicates the steady term, whereas putting Δ indicates the unsteady term. The steady term is assumed to be $O(1)$, and the unsteady term is assumed to be $O(\varepsilon)$ where the ε refers to a small quantity. Furthermore, it is assumed that η_0 is given, and the unsteady term of u (Δu) is not considered for simplicity. Substituting Eq.(17) to the motion equations Eq.(6), two sets of the motion equations can be obtained for the steady and unsteady terms. It should be mentioned that the motion equations for the steady term coincide with the unsteady ones when we set the acceleration, the angular acceleration, and the angular velocity terms zero in Eq.(6). The motion equations for the unsteady term can be obtained by eliminating the higher order terms of ε in the equations, namely, linearizing the motion equations. Therefore, the ship's course stability can be evaluated based on the linearized motion equations.

In addition to the motion equations, a relationship between η and v_m , expressed as Eq.(5), needs to be considered as the base equation. By substituting Eq.(17) to Eq.(5), the following equation is derived as

$$\dot{\eta} = u_0 \sin \psi_0 + v_0 \cos \psi_0 + \Delta v \cos \psi_0 + \Delta\psi(u_0 \cos \psi_0 - v_0 \sin \psi_0) + O(\varepsilon^2) \quad (18)$$

Using a relationship of $\tan \psi_0 = -v_0/u_0$, the following linear equation is obtained as

$$\Delta \dot{\eta} = \Delta v \cos \psi_0 + \Delta \psi (u_0 \cos \psi_0 - v_0 \sin \psi_0) \quad (19)$$

When considering a ship's course stability in the close proximity to the bank, we have to consider Eq.(19) as one of the base equations. This is a special feature when considering a ship moving in parallel to the bank wall.

2.4.1 Equations for steady sailing condition and its calculation scheme

The equations for the steady sailing condition are expressed as follows:

$$0 = X_H(u_0, v_0, \phi_0) - (1 - t_R)F_N(u_0, v_0, \delta_0) \sin \delta_0 \cos \phi_0 + (1 - t_P)T(u_0, v_0) + X_A(u_0, v_0, \phi_0, \psi_0) \quad (20)$$

$$0 = Y_H(u_0, v_0, \phi_0) - (1 + a_H)F_N(u_0, v_0, \delta_0) \cos \delta_0 \cos \phi_0 + Y_A(u_0, v_0, \phi_0, \psi_0) \quad (21)$$

$$0 = N_H(u_0, v_0, \phi_0) - (x_R + a_H x_H)F_N(u_0, v_0, \delta_0) \cos \delta_0 \cos \phi_0 + N_A(u_0, v_0, \phi_0, \psi_0) \quad (22)$$

$$0 = -Y_{H0}(u_0, v_0, \phi_0)z_{H0} - Y_{H\eta}(u_0, v_0)z_{H\eta} + (1 + a_H)F_N(u_0, v_0, \delta_0) \cos \delta_0 \cos \phi_0 z_R - mg\overline{GM}\phi_0 + K_A(u_0, v_0, \phi_0, \psi_0) \quad (23)$$

Here, F_N is the rudder normal force, T is the propeller thrust, t_P is the thrust deduction factor, t_R is the steering resistance deduction factor, a_H is the rudder force increase factor, x_R is the longitudinal coordinate of the rudder position ($=-0.5L$), and x_H is the longitudinal coordinate of the acting point of the additional lateral force component induced by steering. Eqs.(20) ~ (23) represent a balance among the hull forces, rudder forces, propeller force and external forces due to wind. The unknown variables are u_0 , v_0 , ϕ_0 and δ_0 .

The above-mentioned equations are non-linear, and hence efficient strategies are needed to solve them. Here, we consider a deformation of the equations. More specifically, and by eliminating $F_N \cos \delta_0 \cos \phi_0$ in Eqs.(21) and (22), the following equation is obtained:

$$0 = (x_R + a_H x_H) [Y_H(u_0, v_0, \phi_0) + Y_A(u_0, v_0, \phi_0, \psi_0)] - (1 + a_H) [N_H(u_0, v_0, \phi_0) + N_A(u_0, v_0, \phi_0, \psi_0)] \quad (24)$$

Similarly, by eliminating $F_N \cos \delta_0 \cos \phi_0$ in Eqs.(21) and (23), the following equation is obtained:

$$0 = Y_H(u_0, v_0, \phi_0)z_R - Y_{H0}(u_0, v_0, \phi_0)z_{H0} - Y_{H\eta}(u_0, v_0)z_{H\eta} - mg\overline{GM}\phi_0 + K_A(u_0, v_0, \phi_0, \psi_0) + Y_A(u_0, v_0, \phi_0, \psi_0)z_R \quad (25)$$

Eqs.(24) and (25) are not the function of rudder angle δ_0 . These equations are used as the base equations to be solved.

The Regula-Falsi method is used to provide numerical solutions to non-linear equations. More specifically, the calculation steps are as follows:

1. Set propeller revolution n_P , lateral deviation of the ship η_0 and wind condition.
2. Set initial value of u_0 to solve Eq.(20) by the Regula-Falsi method.

3. Obtain v_0 and ϕ_0 by solving Eqs.(24) and (25). Then, ψ_0 can be calculated by $\psi_0 \equiv \tan^{-1}(-v_0/u_0)$.
4. Obtain δ_0 by solving Eq.(22).
5. Update u_0 in this cycle until Eq.(20) is satisfied.

2.4.2 Linearized motion equations and course stability

The linearized motion equations for the unsteady term and Eq.(19) are expressed as follows:

$$[A]\{\dot{x}\} = [B]\{x\} + \{d\}\Delta\delta \quad (26)$$

where

$$[A] = \begin{bmatrix} a_1 & a_2 & a_3 & 0 & 0 & 0 \\ a_4 & a_5 & a_6 & 0 & 0 & 0 \\ a_7 & a_8 & a_9 & 0 & 0 & 0 \\ 0 & 0 & 0 & 1 & 0 & 0 \\ 0 & 0 & 0 & 0 & 1 & 0 \\ 0 & 0 & 0 & 0 & 0 & 1 \end{bmatrix}, \quad [B] = \begin{bmatrix} b_1 & b_2 & b_3 & b_4 & b_5 & b_6 \\ b_7 & b_8 & b_9 & b_{10} & b_{11} & b_{12} \\ b_{13} & b_{14} & b_{15} & b_{16} & b_{17} & b_{18} \\ b_{19} & 0 & 0 & 0 & b_{20} & 0 \\ 0 & 1 & 0 & 0 & 0 & 0 \\ 0 & 0 & 1 & 0 & 0 & 0 \end{bmatrix} \quad (27)$$

$$\{x\} = \begin{Bmatrix} \Delta v \\ \Delta r \\ \Delta \dot{\phi} \\ \Delta \eta \\ \Delta \psi \\ \Delta \phi \end{Bmatrix}, \quad \{d\} = \begin{Bmatrix} d_1 \\ d_2 \\ d_3 \\ 0 \\ 0 \\ 0 \end{Bmatrix} \quad (28)$$

In $[A]$, $[B]$ and $\{d\}$ matrices, $a_1 \sim a_9$, $b_1 \sim b_{20}$ and $d_1 \sim d_3$ are expressed as follows:

$$\begin{aligned} a_1 &= m + m_y \\ a_2 &= x_G m \\ a_3 &= -(m_y \alpha_z + m z_G) \\ a_4 &= x_G m \\ a_5 &= I_{zz} + J_{zz} + m x_G^2 \\ a_6 &= -m z_G x_G \\ a_7 &= -(m_y \alpha_z + m z_G) \\ a_8 &= -m z_G x_G \\ a_9 &= I_{xx} + J_{xx} + m z_G^2 \end{aligned}$$

$$\begin{aligned} b_1 &= F_{Hv1} + F_{Rv1} + F_{Av1} \\ b_2 &= -(m + m_x)u_0 + F_{Hr1} + F_{Rr1} \\ b_3 &= F_{R\dot{\phi}1} \\ b_4 &= F_{H\eta1} \end{aligned}$$

$$\begin{aligned}
b_5 &= F_{A\psi 1} + F_{W\psi 1} \\
b_6 &= F_{H\phi 1} + F_{R\phi 1} + F_{A\phi 1} \\
b_7 &= F_{Hv 2} + F_{Rv 2} + F_{Av 2} \\
b_8 &= -mx_G u_0 + F_{Hr 2} + F_{Rr 2} \\
b_9 &= F_{R\dot{\phi} 2} \\
b_{10} &= F_{H\eta 2} \\
b_{11} &= F_{A\psi 2} + F_{W\psi 2} \\
b_{12} &= F_{H\phi 2} + F_{R\phi 2} + F_{A\phi 2} \\
b_{13} &= F_{Hv 3} + F_{Rv 3} + F_{Av 3} \\
b_{14} &= mz_G u_0 + F_{Hr 3} + F_{Rr 3} \\
b_{15} &= F_{R\dot{\phi} 3} + K_{\dot{\phi}} \\
b_{16} &= F_{H\eta 3} \\
b_{17} &= F_{A\psi 3} + F_{W\psi 3} \\
b_{18} &= F_{H\phi 3} + F_{R\phi 3} + F_{A\phi 3} \\
b_{19} &= \cos \psi_0 \\
b_{20} &= u_0 \cos \psi_0 - v_0 \sin \psi_0
\end{aligned}$$

$$\begin{aligned}
d_1 &= F_{R\delta 1} \\
d_2 &= F_{R\delta 2} \\
d_3 &= F_{R\delta 3}
\end{aligned}$$

When the first subscript in F appears in the above-mentioned equations, H refers to the hull hydrodynamic forces, R refers to the rudder forces, and A refers to the wind forces. The second subscript in F refers to the parameter for partial differential, and the third subscript number 1, 2 and 3 refer to the lateral force, yaw moment and roll moment, respectively. For instance, F_{Hvi} ($i = 1, 2, 3$) mean as:

$$\begin{aligned}
F_{Hv1} &\equiv \frac{\partial Y_H}{\partial v} \\
F_{Hv2} &\equiv \frac{\partial N_H}{\partial v} \\
F_{Hv3} &\equiv \frac{\partial K_H}{\partial v} = -z_{H0} \frac{\partial Y_{H0}}{\partial v} - z_{H\eta} \frac{\partial Y_{H\eta}}{\partial v}
\end{aligned}$$

These can be calculated analytically.

Consider that the ship is moving in the presence of external disturbances using an autopilot. Then, $\Delta\delta$ is assumed to be expressed as follows:

$$\begin{aligned}
\Delta\delta &= -G_1 \Delta\psi - G_2 \Delta r \\
&= [G]\{x\}
\end{aligned} \tag{29}$$

where $[G] = (0, -G_2, 0, 0, -G_1, 0)$. G_1 and G_2 are called control gains. Consequently, the motion equation, Eq.(26) can be rewritten as follows:

$$\{\dot{x}\} = [A]^{-1} ([B] + \{d\}[G]) \{x\} \tag{30}$$

Thus, the unsteady terms $\{x\}$ can be calculated by $[A]^{-1}([B] + \{d\}[G])$ as shown in Eq.(30). If we obtain the eigenvalues of square matrix of 6×6 of $[A]^{-1}([B] + \{d\}[G])$, we can easily assess whether the target ship is stable or not for course keeping. The motion becomes stable when all parts of the real eigenvalues are negative, and the motion becomes unstable when even one part is positive.

3 Studied Ship

3.1 Principal particulars

A pure car carrier (PCC) was selected as a case study in this paper[7]. Table 1 shows the principal particulars of the PCC. The load condition is full load, even keel. In this table, B denotes the breadth, ∇ denotes the displacement volume, x_G denotes the longitudinal position of center of gravity (fore position from the midship is considered positive), C_b denotes the block coefficient, D_P denotes the propeller diameter, $A_R/(Ld)$ denotes the rudder area ratio, H_R denotes the rudder span length, and A_X and A_Y denote front and side profile areas of the ship in air, respectively. Radius of yaw gyration k_{zz} is assumed to be $0.25L$. Fig.2 shows the side profile of the PCC[11], and Fig.3 shows the body plan of the ship.

Table 1: Principal particulars of a PCC

items	value
L (m)	180.00
B (m)	32.20
d (m)	8.20
∇ (m ³)	26000
x_G (m)	-2.53
C_b	0.547
\overline{GM} (m)	1.25
\overline{KM} (m)	15.60
D_P (m)	6.00
$A_R/(Ld)$	1/39.5
H_R (m)	7.200
A_X (m ²)	859
A_Y (m ²)	4387

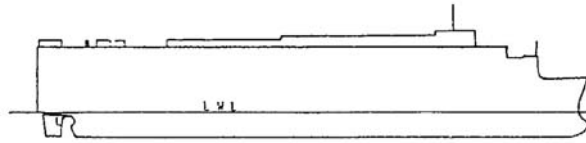


Fig. 2: Ship profile of a PCC

3.2 Main engine

Table 2 demonstrates the main engine specifications . As the base engine of the PCC, we selected that engine power at Maximum Continuous Rating (P_{MCR}) is 11,000 kW, and the propeller revolution at MCR (N_{MCR}) is 105 rpm. The design speed (V_S) is 20 kn. Furthermore, P_S is the engine power at Normal Rating (NOR) with 15% sea margin,

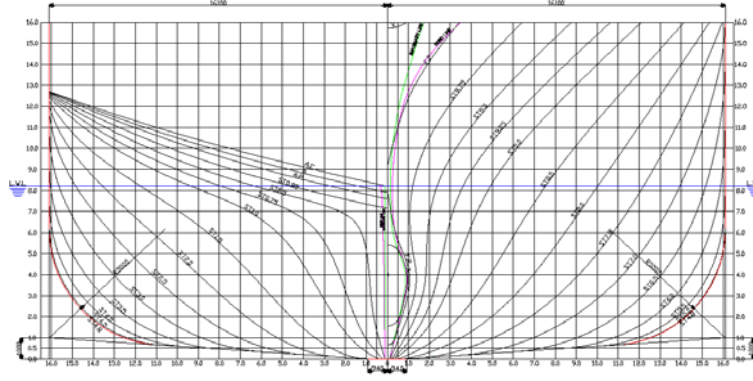


Fig. 3: Body plan of a PCC

and N_S is the propeller revolution at P_S . Q_{EMAX} is the maximum torque for the main engines, which was obtained using the following formula: $Q_{EMAX} = P_{MCR}/(2\pi N_{MCR})$. Note that this engine is a virtual one, and hence full-scale ships with this type of engine do not exist in reality. The same propeller is used for this ship as the propeller designed in the previous study[7].

Table 2: Specification of main engines

symbol	value
P_{MCR} (kW)	11,000
N_{MCR} (rpm)	105
P_S (kW)	8,287
N_S (rpm)	92
Q_{EMAX} (ton-m)	107

3.3 Hydrodynamic derivatives and parameters

This sub-section presents the hydrodynamic force derivatives and parameters used for the calculation of SSC and the CS in shallow water. Tables 3 and 4 show the hydrodynamic derivatives and coefficients, respectively. The roll-related derivatives were obtained by the captive model tests by varying the respective heel angles[5]. The derivatives related to $\eta'(\equiv \eta/L)$ (bank-related derivatives) were also obtained by the captive model tests in shallow water[5]. The derivatives and virtual mass coefficients, except from the roll-related and the bank-related derivatives mentioned above, and the interaction coefficients (t_P , t_R , a_H , x'_H) shown in Table 4 were obtained by the captive model tests in shallow water by Yoshimura[12]. The radius of roll gyration k_{xx} in Table 3 was obtained by the roll decay test. Note that k_{xx} includes the added moment of inertia with respect to the roll. z_{H0} and $z_{H\eta}$ were obtained from the lateral force and roll moment measured by the captive model tests[5]. z_R was assumed as a half position of the rudder span.

Table 3: Hydrodynamic derivatives and other coefficients used in the calculations

h/d	1.5	1.2	h/d	1.5	1.2
Y'_v	-0.993	-2.314	N'_v	-0.2043	-0.4620
Y'_r	0.0934	0.2089	N'_r	-0.0689	-0.1286
Y'_{vvv}	-5.03	-1.70	N'_{vvv}	-0.308	-0.914
Y'_{vvr}	1.71	7.88	N'_{vvr}	-1.874	0.003
Y'_{vrr}	-1.992	-3.042	N'_{vrr}	-0.0686	0.0880
Y'_{rrr}	-0.1246	-0.1542	N'_{rrr}	-0.1495	-0.1469
Y'_ϕ	0.0444	0.1443	N'_ϕ	-0.0591	-0.1080
$Y'_{v\phi}$	2.966	4.699	$N'_{v\phi}$	-0.8497	0.1825
$Y'_{v\phi\phi}$	-3.749	-7.715	$N'_{v\phi\phi}$	-0.6035	-1.947
$Y'_{r\phi\phi}$	0.739	2.533	$N'_{r\phi\phi}$	0.4444	1.315
$Y'_{rr\phi}$	0.8969	2.264	$N'_{rr\phi}$	0.0189	0.2669
Y'_η	0.009	0.028	N'_η	-0.012	-0.039
$Y'_{\eta\eta\eta}$	0.738	0.679	$N'_{\eta\eta\eta}$	-0.154	-0.344
$Y'_{vv\eta}$	-0.585	0.721	$N'_{vv\eta}$	-1.307	-1.923
$Y'_{v\eta\eta}$	-0.718	-0.293	$N'_{v\eta\eta}$	-0.056	0.031
X'_{vv}	0.0460	0.3178	$m' + m'_x$	0.232	0.301
X'_{vr}	0.297	0.467	$m' + m'_y$	0.413	0.544
X'_{rr}	-0.0069	0.0038	$I'_{zz} + J'_{zz}$	0.0262	0.0293
X'_{vvvv}	0.718	0.574	k_{xx}/B	0.31	0.32
$X'_{v\phi}$	0.0046	-0.3804	z_{H0}/d	-0.15	-0.29
$X'_{r\phi}$	-0.0863	-0.0611	$z_{H\eta}/d$	1.01	0.59
$X'_{\phi\phi}$	0.0647	0.1213	z_R/d	0.57	0.57
$X'_{\eta\eta}$	-0.040	-0.066			
$X'_{v\eta}$	-0.036	-0.087			

Table 4: Interaction coefficients used for the calculations

h/d	1.5	1.2
t_P	0.227	0.305
t_R	0.262	0.224
a_H	0.710	0.875
x'_H	-0.341	-0.322

3.4 Bank effect on added mass coefficients

The potential theory is used to investigate the bank effect on the added mass by systematically changing the lateral deviation of the ship η . The added mass was calculated by solving the base equation[13] on the assumption of a rigid wall free-surface. The source distribution was used for both the bank and the ship hull surface[15]. The effect of the water depth was considered taking the mirror images of the source-terms both vertically and infinitely [14].

Fig.4 exhibits the calculations of m_x/m_{x0} , m_y/m_{y0} and J_{zz}/J_{zz0} as a function of $\eta/L(=\eta')$. Here, m_x , m_y and J_{zz} denote the added mass for surge, the added mass for sway and the added moment of inertia for yaw, respectively, when the ship is moving on the straight line of $y = \eta$. Similarly, m_{x0} , m_{y0} and J_{zz0} denote the added mass when a ship is moving on the straight line of $y = 0$ and the bank effect disappears. In the case of $h/d = 1.5$, m_x/m_{x0} , m_y/m_{y0} and J_{zz}/J_{zz0} are almost constant and the values are almost one even in cases where η' becomes significantly large and reaches the bank. On the contrary, in the case of $h/d = 1.2$, m_x/m_{x0} , m_y/m_{y0} and J_{zz}/J_{zz0} they all change when increasing η' approximately 18% in maximum. Thus, in the extreme shallow water case such as $h/d = 1.2$, the bank effect on the added mass becomes significant and has to be considered in the subsequent motion simulations.

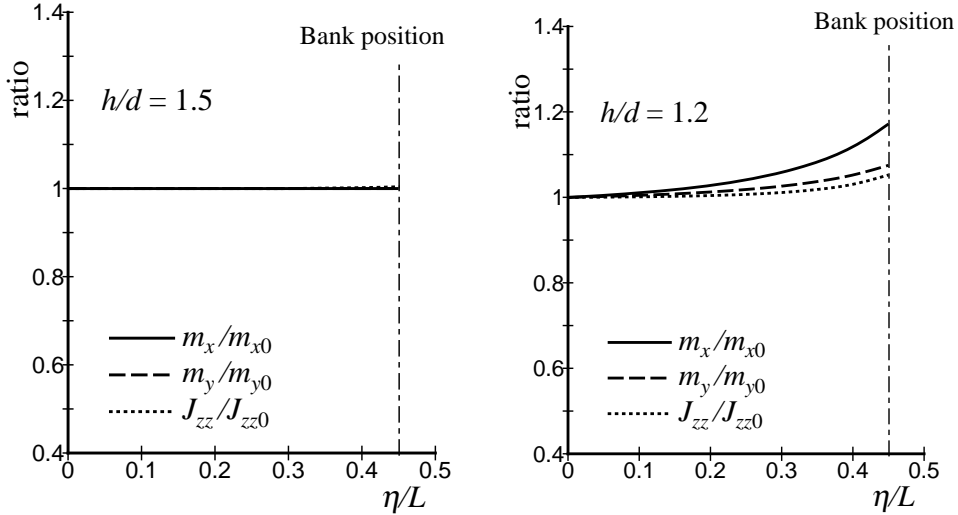


Fig. 4: Calculation results of added mass ratios of a ship close to a bank

4 Steady Sailing Condition of a Ship Close to a Bank in No Wind Condition

First, we consider the SSC of a ship moving in the close proximity to a bank under no wind condition. Here, the water depth h changes to 12.30 m and 9.84 m in full-scale, which are, in turn, expressed in a non-dimensional form as $h/d = 1.5$ and $h/d = 1.2$, respectively. The distance between the x_0 -axis fixed to the space and the bank toe at the bottom W (see Fig.1) is assumed to be $0.45L$ (81 m in full-scale). The position where the lateral deviation of the ship centerline η_0 is zero, suggests that the bank effect vanishes. The main engine is supposed to be the condition of “HALF” with the propeller revolution $N_P = 44$ rpm where the ship sails with 10 kn in calm and deep water.

Fig.5 exhibits the calculations of the check helm δ_0 , the hull drift angle β_0 , the ship speed U_0 and the heel angle ϕ_0 versus η_0/L . For reference purposes, we have also plotted the results using simplified formulas[5] for the check helm (δ_0) and the hull drift angle (β_0) as:

$$\delta_0 = \eta'_0 \frac{Y_\eta^{*'} N_v^{*'} - N_\eta^{*'} Y_v^{*'}}{Y_v^{*'} N_\delta^{*'} - N_v^{*'} Y_\delta^{*'}} = -\eta'_0 \frac{Y_\eta^{*'} l'_v - l'_\eta}{Y_\delta^{*'} l'_v - l'_\delta} \quad (31)$$

$$\beta_0 = \eta'_0 \frac{Y_\eta^{*'} N_\delta^{*'} - N_\eta^{*'} Y_\delta^{*'}}{Y_v^{*'} N_\delta^{*'} - N_v^{*'} Y_\delta^{*'}} = \eta'_0 \frac{Y_\eta^{*'} l'_\delta - l'_\eta}{Y_v^{*'} l'_\delta - l'_v} \quad (32)$$

where

$$\left. \begin{aligned} Y_v^{*'} &= Y_v' + Y_{v\eta\eta}' \eta_0'^2 \\ N_v^{*'} &= N_v' + N_{v\eta\eta}' \eta_0'^2 \\ Y_\eta^{*'} &= Y_\eta' + 3Y_{\eta\eta\eta}' \eta_0'^2 \\ N_\eta^{*'} &= N_\eta' + 3N_{\eta\eta\eta}' \eta_0'^2 \end{aligned} \right\} \quad (33)$$

Here, l'_v is the non-dimensional longitudinal acting point of the hull lateral force in oblique motion ($\equiv N_v^{*'} / Y_v^{*'}$) and l'_η is the longitudinal acting point of the bank suction force ($\equiv N_\eta^{*'} / Y_\eta^{*'}$). l'_δ is non-dimensional longitudinal acting point of the rudder force ($\equiv N_\delta' / Y_\delta'$). Table 5 exhibits the values of Y_δ' and N_δ' used in the analysis. These values were obtained using the captive model data by Yoshimura[12].

Table 5: Rudder force coefficients

h/d	1.5	1.2
Y_δ'	-0.091	-0.100
N_δ'	0.040	0.042

Using this method, δ_0 increases with increasing η_0/L , and this trend becomes more significant when $h/d = 1.2$. However, the check helm is within 35° . On the other hand, β_0 is quite small and its absolute value is less than 1° . U_0 decreases with increasing η_0/L , and this trend becomes more significant when $h/d = 1.2$ due to the increase in the ship resistance. This mainly stems from the negative-value of $X'_{\eta\eta}$ which is the hydrodynamic characteristic of the studied ship as listed in Table 3. This indicates that the

ship resistance increases with increasing η_0 , and this trend becomes more significant when $h/d = 1.2$. The absolute value of ϕ_0 is also quite small because the ship speed is slow.

The calculation result of δ_0 and β_0 using the simplified formulas (denoted as ‘formula’ in the figure) changes in the same way as the exact calculation result (denoted as ‘present’ in the figure) when η_0/L is small. As η_0/L becomes large, the absolute values of δ_0 and β_0 become overestimated, and the difference with the exact calculation results becomes significantly large. Although the rudder force increases due to the propeller load increase concurrent with the speed drop, the simplified calculation does not consider the effect of the speed drop. This is main reason that both δ_0 and β_0 become overestimated. Furthermore, and although the simplified formulas are useful for the assessment of the check helm and the hull drift angle, the exact calculation is necessary to predict both parameters quantitatively.

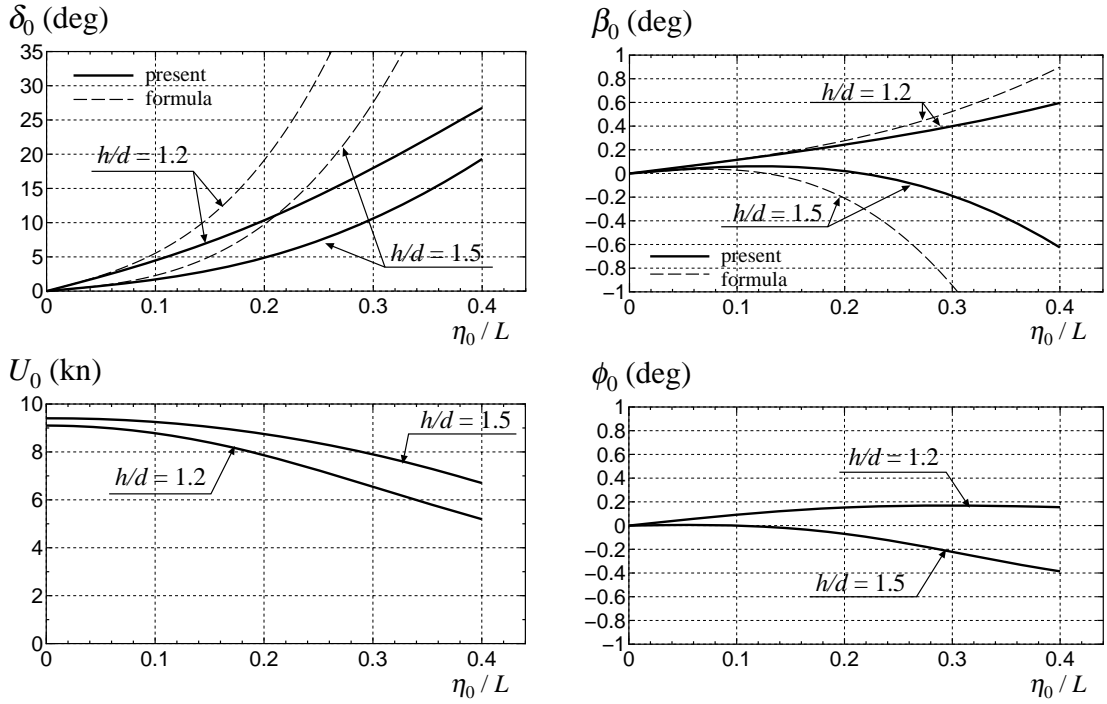


Fig. 5: Calculation results of steady sailing conditions of a ship close to a bank

5 Steady Sailing Performance of a Ship Close to a Bank in Wind

5.1 Calculation conditions

To capture a bank effect on the SSC and CS under windy condition, the lateral deviation of the ship centerline η_0 needs to change as listed in Table 6. In this table, the distance from the bank toe to the ship side s_0 is also shown.

Table 6: Lateral deviation of ship centerline η_0 , and distance from the bank toe to the ship side s_0

η_0 (m)	0.0	36.0	54.0
(η_0/L)	(0.00)	(0.20)	(0.30)
s_0 (m)	64.9	28.9	10.9
(s_0/L)	(0.36)	(0.16)	(0.06)

The main engine is supposed to be in “HALF” condition with a propeller revolution at $N_P = 44$ rpm. This condition is similar to the no wind condition mentioned in the previous section.

5.2 Wind conditions

Table 7 shows the calculations under windy condition. The wind’s strength is measured in Beaufort (BF) Scale. To capture the wind effect on the SSC and the CS, the BF scale is changed as shown in Table 7. The SSC and the CS were calculated by systematically changing the wind direction in the range of $\theta_W = -180^\circ \sim 180^\circ$ for each BF scale.

Table 7: Wind conditions

Beaufort scale	BF6	BF7	BF8	BF9
U_W (m/s)	13.9	17.2	20.8	24.5

The aerodynamic force coefficients (C_{XA} , C_{YA} , C_{NA} , C_{KA}) of the ship were measured by Fujiwara’s method[16] and are shown in Fig.6. The aerodynamic force coefficients are defined as

$$C_{XA} = \frac{X_A}{(1/2)\rho_a A_X V_A^2} \quad (34)$$

$$C_{YA} = \frac{Y_A}{(1/2)\rho_a A_Y V_A^2} \quad (35)$$

$$C_{NA}, C_{KA} = \frac{N_A, K_A}{(1/2)\rho_a A_Y V_A^2 L} \quad (36)$$

Here, ρ_a denotes the air density and V_A denotes the relative wind velocity. The aerodynamic force coefficients are expressed as a function of the relative wind direction θ_A .

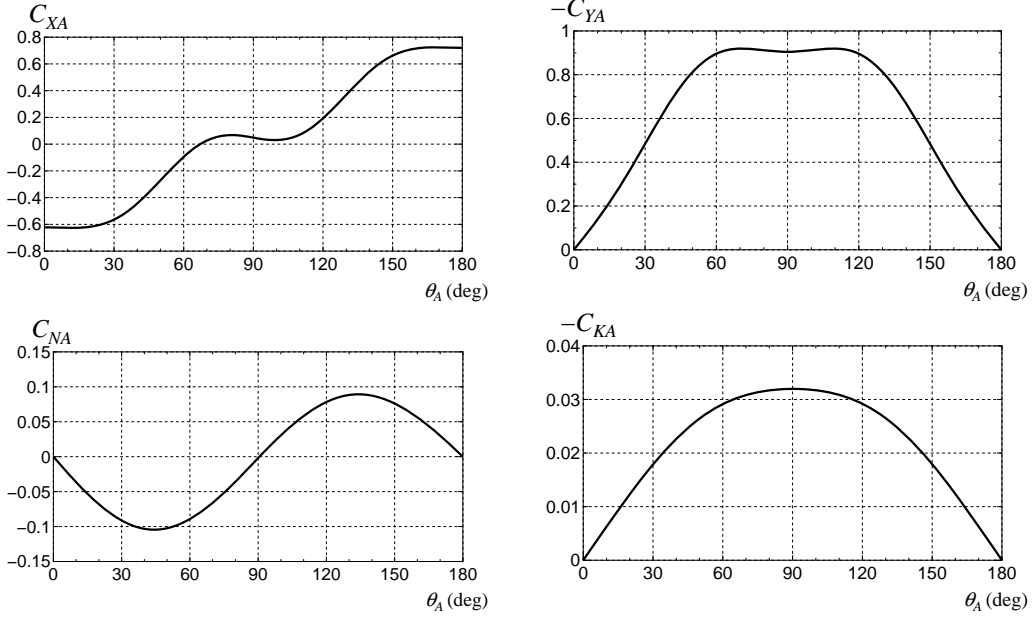


Fig. 6: Aerodynamic force coefficients

5.3 Steady sailing condition

First, we calculated the SSC including the ship speed U_0 , the check helm δ_0 , the hull drift angle β_0 , and the heel angle ϕ_0 of a PCC for different η_0 in $h/d = 1.5$ and 1.2 .

Figs.7 and 8 show the calculation results of U_0 and δ_0 , respectively. Note that the situation when the absolute value of δ_0 is over 35° is considered to be a “no-solution” in which the check helm does not exist. In the following graph, the horizontal axis is the absolute wind direction θ_W . In $\eta_0/L = 0$, the result of U_0 follows a left-right symmetry, and U_0 drops significantly at the head wind direction ($-60^\circ \sim 60^\circ$). In $\eta_0/L = 0.2$ and 0.3 where the ship gets to the close proximity of the bank, the symmetry breaks and U_0 becomes smaller for the wind stemming from the port side ($-180^\circ \sim 0^\circ$). This is because the ship resistance increases in $\eta_0/L = 0.2$ and 0.3 , and this comes from the negative-value of $X'_{\eta\eta}$ as mentioned in section 4. In addition to that, when sailing in the close proximity to the bank, the positive check helm is necessary for efficient course-keeping because the bank suction force acts on the ship as well. As shown in Fig.8, δ_0 shifts vertically upward as η_0/L becomes larger. Generally, δ_0 takes a positive peak at approximately $\theta_W = -120^\circ$ and a negative peak at approximately $\theta_W = 120^\circ$. Therefore, it becomes larger as an entire when the wind stems from $-180^\circ \sim 0^\circ$ due to the bank suction effect. When the absolute value of δ_0 becomes large enough, the increase in resistance due to steering becomes large as well. Consequently, U_0 becomes smaller in wind stemming from $-180^\circ \sim 0^\circ$.

Fig.9 exhibits the calculation results of the hull drift angle β_0 . β_0 is positive when the wind stems from starboard side ($0^\circ \sim 180^\circ$). This underlines that the ship bow heads to the direction of the bank. On the other hand, when the β_0 value is large enough, there is a possibility that the ship bow will touch the bank wall, and this situation is very dangerous. The peak value of β_0 at approximately $\theta_W = 35^\circ$ becomes significantly important when discussing navigation safety. The peak value of $h/d = 1.2$ is slightly lower than that in $h/d = 1.5$. This is because the absolute value of the sway hydrodynamic derivative Y'_v

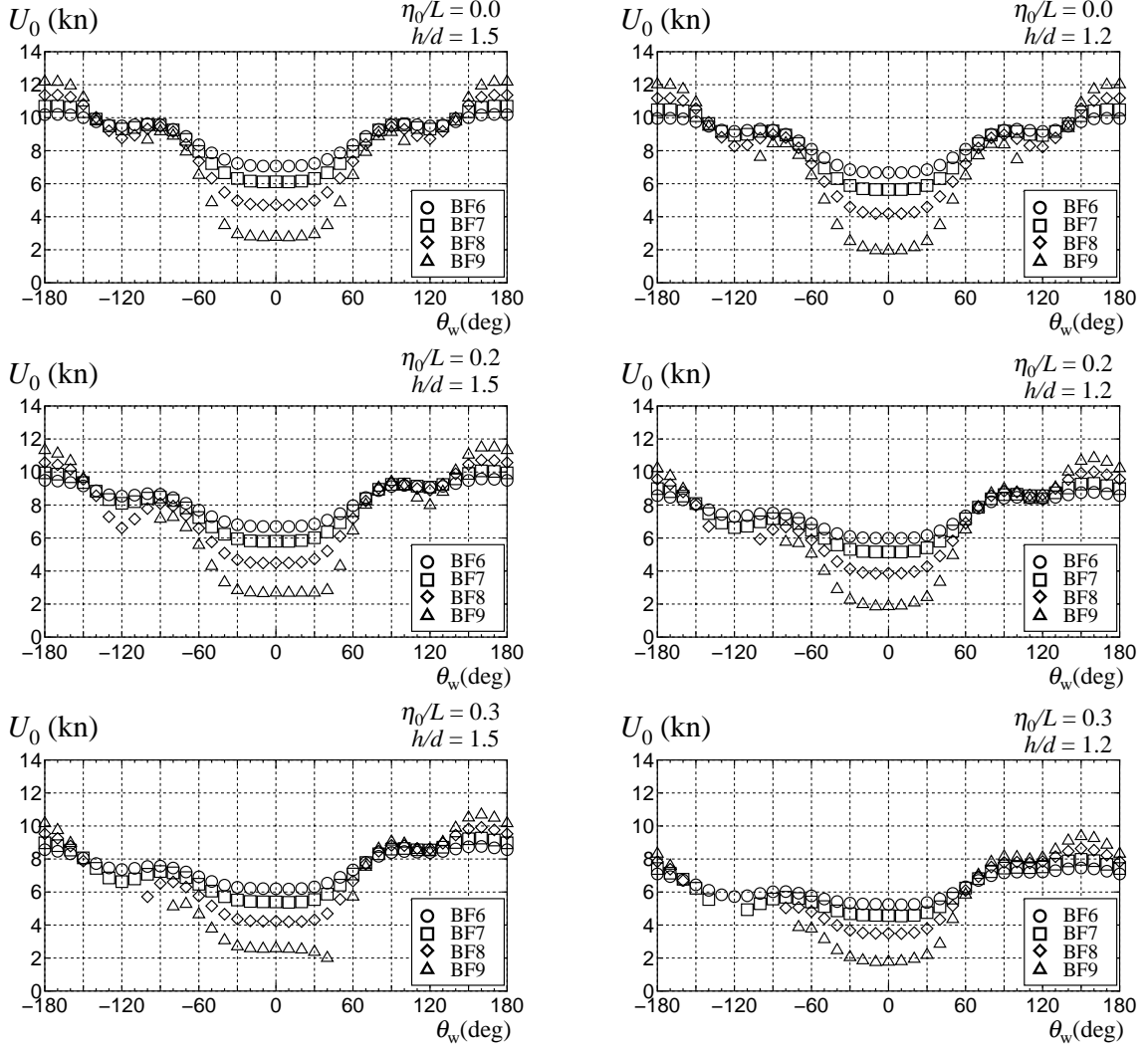


Fig. 7: Ship speed (U_0) in the different η_0 (left: $h/d = 1.5$, right: $h/d = 1.2$)

increases in more shallow water depth (see Table 3). It is considered that increased sway damping force (the large absolute value of Y'_v) induces a decrease in the peak value of β_0 .

Fig.10 shows the calculation results of the heel angle ϕ_0 . ϕ_0 takes a peak at almost $\theta_w = 110^\circ$, and its maximum absolute value is approximately 2° . Its order of magnitude is significantly low because the ship's speed is relatively slow.

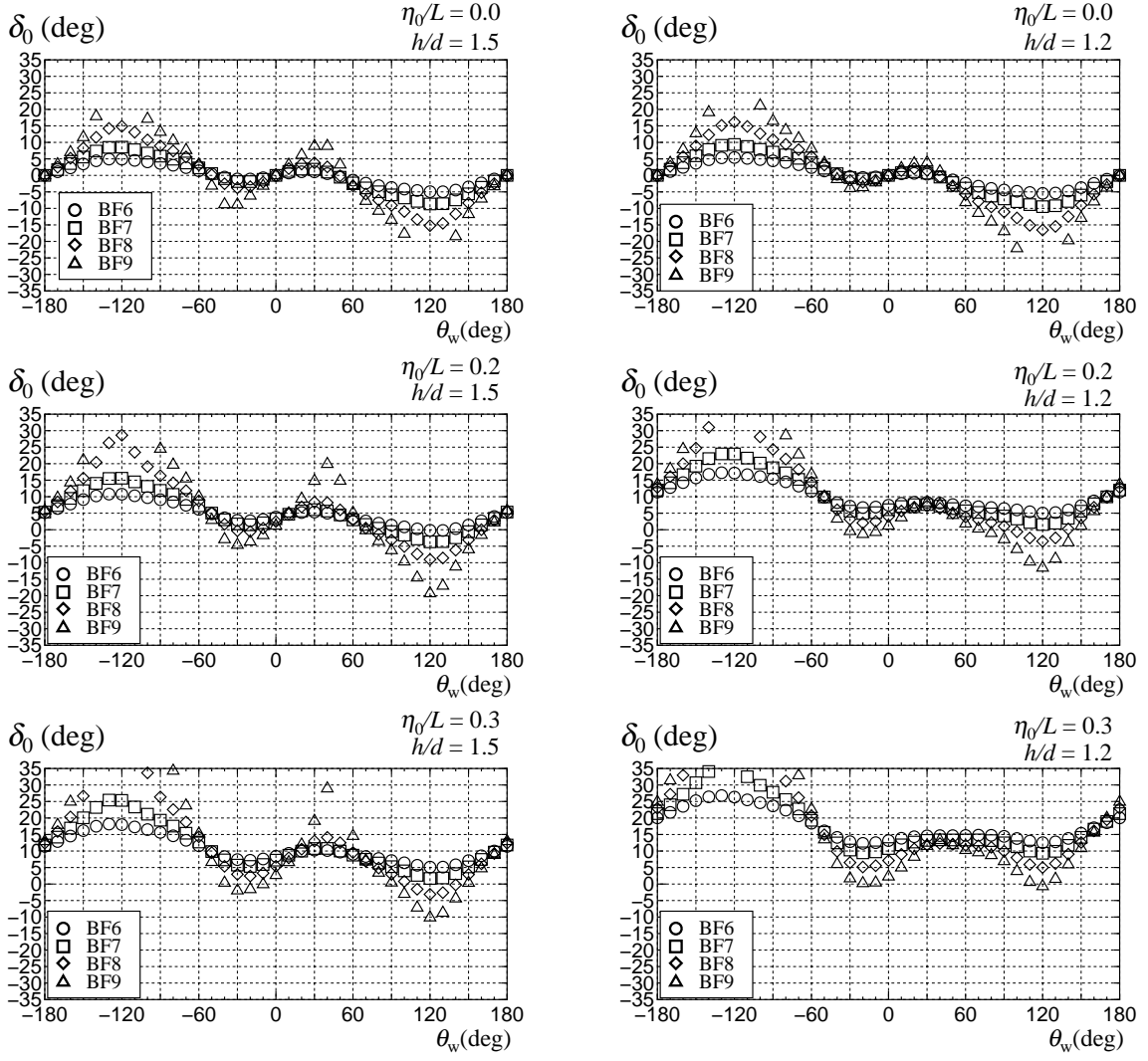


Fig. 8: Check helm (δ_0) in the different η_0 (left: $h/d = 1.5$, right: $h/d = 1.2$)

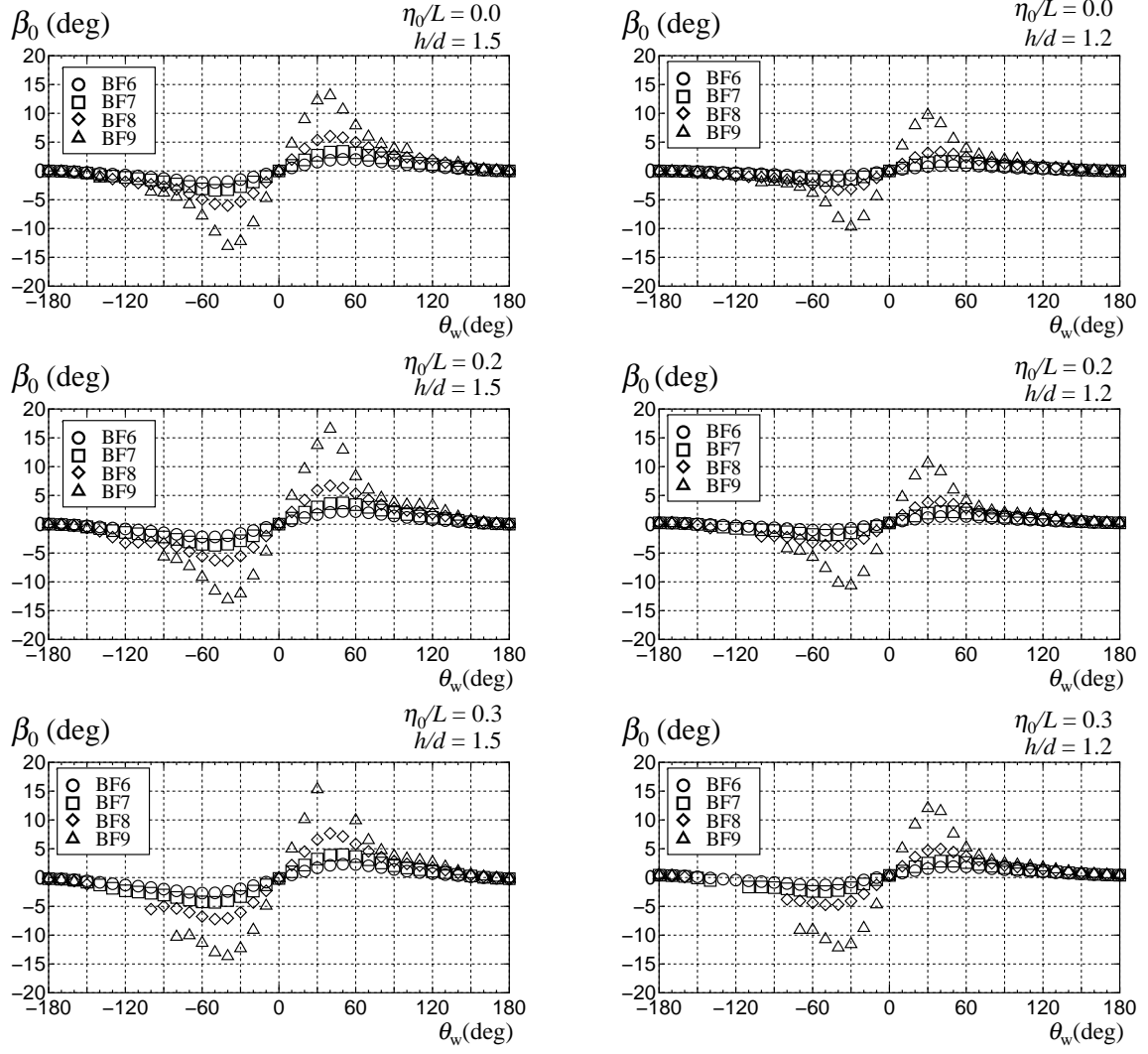


Fig. 9: Hull drift angle (β_0) in the different η_0 (left: $h/d = 1.5$, right: $h/d = 1.2$)

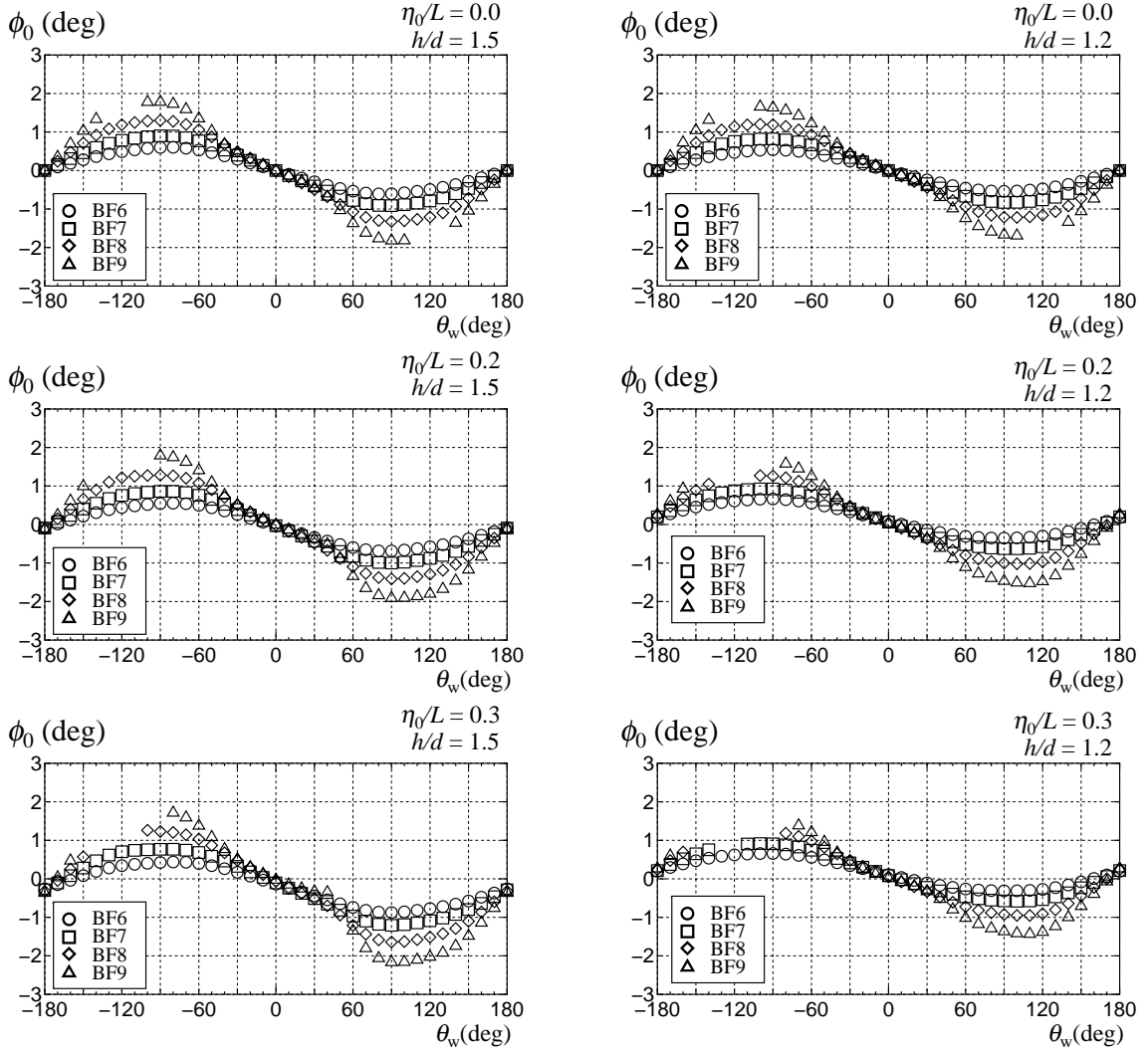


Fig. 10: Heel angle (ϕ_0) in the different η_0 (left: $h/d = 1.5$, right: $h/d = 1.2$)

5.4 Course stability

Next, we consider the course stability. To investigate the effect of control gain (G_1, G_2) and of the autopilot on the course stability, the gains are changed as follows:

1. $(G_1, G_2) = (0, 0)$
2. $(G_1, G_2) = (3, 30 \text{ s})$

Figs.11 and 12 show the calculated results of the CS in $h/d = 1.5$ and $h/d = 1.2$. In these figures, the radius from the origin represents the BF scale and the angle from the vertical axis refers to the wind direction (θ_W). In the concrete, the vertical upward direction is 0° , the vertical downward direction is 180° or -180° , a horizontal direction to the right is 90° and the horizontal direction to the left is -90° . In the following graph, a circle represents stability for course keeping, whereas a black square represents instability. Furthermore, we plotted '*' to provide us with a 'No solution' when the solution cannot be obtained numerically, and hence the check helm has exceeded 35° in the calculation process.

When $\eta_0/L = 0$, then the ship becomes dynamically unstable in head and following wind directions, provided that the control gains are zero. This trend is similar to the result acquired for the course stability in ships under windy condition [17][18][7]. Points of 'No solution' appear in BF9 ranging between $110^\circ \sim 130^\circ$ and $-110^\circ \sim -130^\circ$ for θ_W in both $h/d = 1.5$ and 1.2 . The ship becomes completely stable when applying the control with $(G_1, G_2) = (3, 30 \text{ s})$. In $\eta_0/L = 0.2$, the ship becomes unstable in almost all wind directions, provided that the control gains are zero. On the other hand, points of 'No solution' appear in BF8 and BF9 ranging between $-100^\circ \sim -150^\circ$ for θ_W in both $h/d = 1.5$ and 1.2 . Moreover, in $\eta_0/L = 0.3$, 'No solution' appears in BF8 and BF9 ranging between $-80^\circ \sim -150^\circ$ for θ_W in $h/d = 1.5$, and in BF7 \sim BF9 with the range of $-70^\circ \sim -160^\circ$ in $h/d = 1.2$. It should also be mentioned that the area of 'No solution' increases in the negative θ_W . When the control gain is $(G_1, G_2) = (3, 30 \text{ s})$, then the ship becomes stable except for BF9. Thus, the bank effect on the course stability is significant, and the presence of the bank renders the ship more unstable under windy condition.

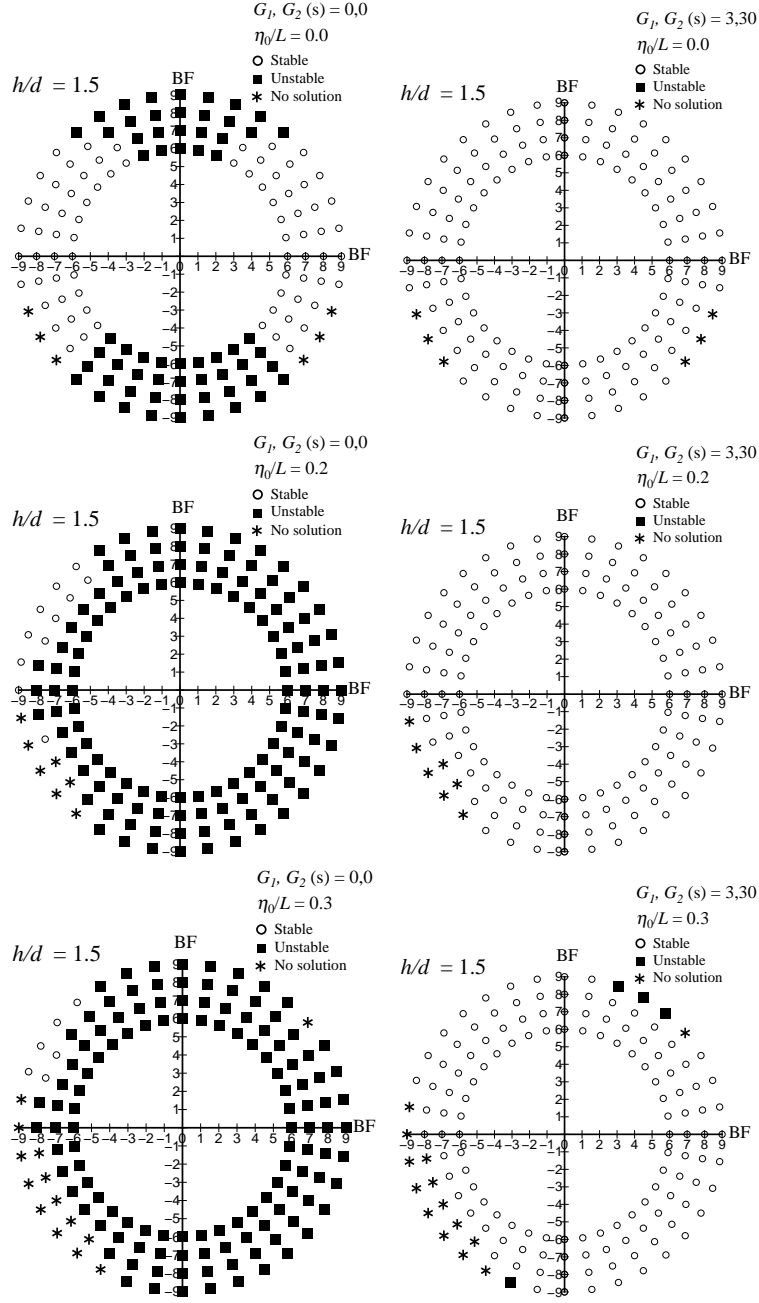


Fig. 11: Effect of control gain on course stability in the different η_0 ($h/d = 1.5$)

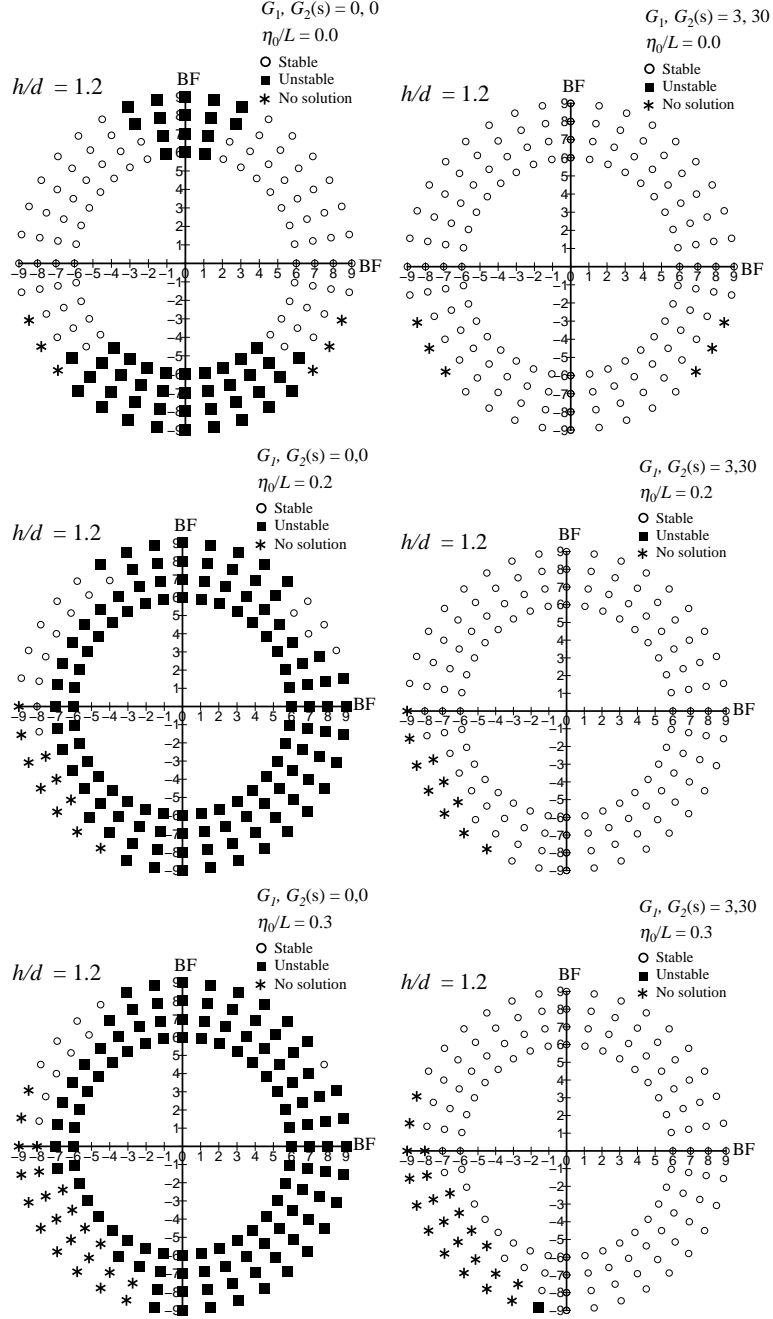


Fig. 12: Effect of control gain on course stability in the different η_0 ($h/d = 1.2$)

5.5 Maneuvering limit

Based on the above, this section evaluates the ship's maneuvering limit under steady wind. However, and to evaluate the maneuvering limit in detail, the following parameters are assumed to ensure that the ship can sail safely while maintaining its course:

C1: The ship speed U_0 is more than 4 kn.

C2: The torque rich does not occur. (The propeller torque Q is less than 107 ton-m)

C3: The absolute value of check helm δ_0 is less than 35° .

C4: The hull drift angle β_0 is less than

- 30° in $\eta_0/L = 0$
- 18° in $\eta_0/L = 0.2$
- 7° in $\eta_0/L = 0.3$

C5: The absolute value of the heel angle ϕ_0 is less than 5° .

C6: Dynamic stability is assumed in course keeping. (The control gains for the autopilot are assumed to be $G_1 = 3$ and $G_2 = 30$ s).

For C4, the limiting values with respect to β_0 change with η_0/L because the ship's bow may touch the bank wall when it gets too close to the bank. 18° in $\eta_0/L = 0.2$ and 7° in $\eta_0/L = 0.3$ are the hull drift angle when the ship bow actually touches the bank wall.

If all the above conditions are satisfied in all wind directions under a certain BF scale, we can then consider that the ship can navigate safely in the BF scale. If not, then this means that the BF scale is the limiting wind condition. This condition is determined as the maneuvering limit.

Fig.13 shows the ship's unsafe points for three different η_0 . ϕ_0 never exceeds the limiting value assumed. Moreover, torque rich never occurs because the engine output is set at 'Half'. In summary, the present ship satisfies the conditions of C2 and C5. Therefore, the only problems involve the C1 (minimum speed is 4 kn), C3 (maximum rudder angle is 35°), C4 (limit of hull drift angle) and C6 (stable in course keeping) conditions.

In case of $\eta_0/L = 0$, U_0 becomes less than 4 kn in head wind of BF9 ($-40^\circ \sim 40^\circ$). When considering oblique following wind ($110^\circ \sim 130^\circ$) and ($-110^\circ \sim -130^\circ$) of BF9, we cannot obtain the steady solution because the absolute value of δ_0 is greater than 35° in that region. Therefore, the maneuvering limit becomes BF8 in both $h/d = 1.5$ and 1.2 . In case of $\eta_0/L = 0.2$, U_0 becomes less than 4 kn in head wind ($-50^\circ \sim 40^\circ$) of BF9. In oblique following wind from the port side ($-100^\circ \sim -150^\circ$) of BF8 and 9, we cannot obtain the steady solution. On the contrary, there is no issue when considering oblique following wind from the starboard side, although we cannot obtain the steady solution in case of $\eta_0/L = 0$. The maneuvering limit is BF7 in both $h/d = 1.5$ and 1.2 . In case of $\eta_0/L = 0.3$, U_0 becomes less than 4 kn in head wind ($-50^\circ \sim 40^\circ$) of BF9 for $h/d = 1.5$, and ($-60^\circ \sim 40^\circ$) of BF8 and 9 for $h/d = 1.2$. In beam and oblique following wind from the port side ($-80^\circ \sim -150^\circ$) of BF8 and 9 for $h/d = 1.5$, and ($-70^\circ \sim -160^\circ$) of BF7, 8 and 9 for $h/d = 1.2$, we cannot obtain the steady solution. In oblique head wind from

the starboard side ($20^\circ \sim 70^\circ$), β_0 of BF9 becomes greater than 7° . More specifically, there are wind directions for which β_0 becomes larger than 7° even in BF8. Also, several unstable points appear in BF9. The maneuvering limit is BF7 in $h/d = 1.5$ and BF6 in $h/d = 1.2$.

In summary, when the ship moves in close proximity to the bank, which may occur for the starboard side of the ship, we need to consider the following:

1. In case of head wind, the remarkable speed drop appears. In oblique head wind from the starboard side, the hull drift angle increases significantly and there is a possibility that the ship bow touches the bank wall.
2. In oblique following wind condition from the starboard side, the ship can in general sail safely.
3. In oblique following wind condition from the port side, the check helm increases significantly because the wind force adds to the bank suction force. This becomes significant the closer the ship moves to the bank and in more shallow water depth.

Table 8 exhibits the final maneuvering limit of the PCC in proximity to the bank under windy condition.

Table 8: Final maneuvering limit of a PCC in proximity to the bank under windy condition

h/d	1.5	1.2
$\eta_0/L = 0.0$	BF8	BF8
$\eta_0/L = 0.2$	BF7	BF7
$\eta_0/L = 0.3$	BF7	BF6

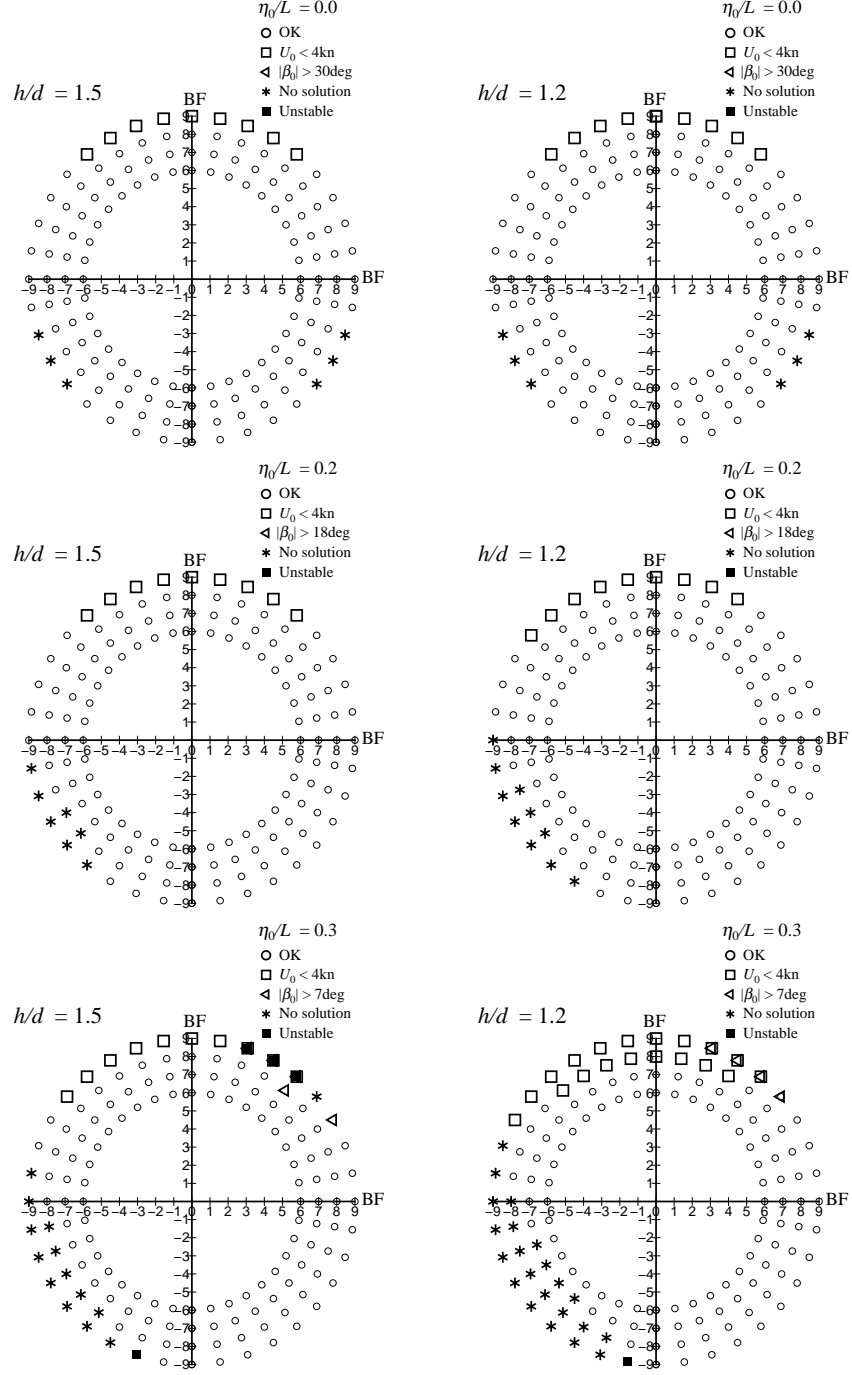


Fig. 13: Maneuvering limit for different values of η_0 (left: $h/d = 1.5$, right: $h/d = 1.2$)

6 Concluding Remarks

This paper presents a method to calculate the steady sailing condition (SSC) including parameters such as check helm, speed drop, hull drift angle etc. of a ship moving in parallel to a bank wall under steady wind, together with the course stability (CS) at the SSC. More specifically, we investigated using this method the bank effect on the SSC and the CS of a 180-m pure car carrier (PCC) under steady wind and we determined the limiting environmental condition for safe navigation (maneuvering limit).

It was initially assumed that the bank exists to the starboard side of the ship. Our findings suggest the following:

- In case of head wind, a significant speed drop appears. In case of oblique head wind from the port side, the hull drift angle increases significantly and there is a distinct possibility that the ship bow will touch the bank wall. In case of oblique following wind condition from the port side, the check helm increases significantly because the wind force adds to the bank suction force. This becomes critical the closer the ship moves to the bank and in more shallow water area.
- In case of no bank, the maneuvering limit of the PCC is BF8 (wind speed 20.8 m/s). In case of $\eta_0/L = 0.2$ ($s_0/L = 0.16$), the maneuvering limit is BF7 (wind speed 17.2 m/s). In case of $\eta_0/L = 0.3$ ($s_0/L = 0.06$), the maneuvering limit is BF7 (wind speed 17.2 m/s) in $h/d = 1.5$ and BF6 (wind speed 13.9 m/s) in $h/d = 1.2$. Thus, the maneuvering limit level becomes severe the closer the ship gets to the bank and in more shallow waters.

Conclusively, the method presented in this paper is a useful tool to assess and quantify the maneuvering limit of the ship moving in close proximity to the bank under steady wind.

The results with respect to the maneuvering limit were obtained under the conditions mentioned in sub-section 5.5 (C1 \sim C6), for the limiting value of the check helm, ship velocity, hull drift angle, heel angle, etc. To study the maneuvering limit extensively, the reliable base conditions of the limiting value must be examined carefully, because the maneuvering limit depends on the base conditions. Further investigation on this is required in future works.

Acknowledgements

This study was supported by the JSPS KAKENHI Grant Number JP26249135. The author expresses his sincere gratitude to Mr. R. Sakuno for his assistance with the captive model tests in shallow water.

References

- [1] Fujino, M. (1968): Experimental Studies on Ship Manoeuvrability in Restricted Waters – Part I, International Shipbuilding Progress, Vol.15, No.168, pp.279-301.
- [2] Fujino, M. (1970): Experimental Studies on Ship Manoeuvrability in Restricted Waters – Part II, International Shipbuilding Progress, Vol.17, No.186, pp.45-65.

- [3] Eda, H. (1971): Directional Stability and Control of Ships in Restricted Channels, Trans. SNAME, Vol.79, pp.71-116.
- [4] Sano, M., Yasukawa, H. and Hata, H. (2014): Directional Stability of a Ship in Close Proximity to Channel Wall, J. Marine Science and Technology, Vol.19, No.4, pp.376-393.
- [5] Yasukawa, H. (2019): Maneuvering Hydrodynamic Derivatives and Course Stability of a Ship Close to Bank, Ocean Engineering (in press).
- [6] Yasukawa, H., Sano, M. and Amii, H. (2013): Wind Effect on Directional Stability of a Ship Moving in a Channel, J. Japan Society of Naval Architects and Ocean Engineers, Vol.18, pp.45-53 (in Japanese).
- [7] Yasukawa, H. and Sakuno, R. (2019): Application of the MMG-Method for Prediction of Steady Sailing Condition and Course Stability of a Ship under External Disturbances, J. Marine Science and Technology (in press).
- [8] Hamamoto, M. and Kim, Y. (1993): A New Coordinate System and the Equations Describing Manoeuvring Motion of a Ship in Waves, J. Society of Naval Architects of Japan, Vol.173, pp.209-220 (in Japanese).
- [9] Yasukawa, H., Sakuno, R. and Yoshimura, Y. (2019): Practical Maneuvering Simulation Method of Ships Considering the Roll-Coupling Effect, J. Marine Science and Technology, Vol.24, 1280-1296.
- [10] Yasukawa, H. and Yoshimura, Y. (2015): Introduction of MMG Standard Method for Ship Maneuvering Predictions, J. Marine Science and Technology, Vol.20, No.1, pp.37-52.
- [11] Yoshimura, Y. and Nagashima, J. (1985): Estimation of the Manoeuvring Behavior of Ship in Uniform Wind, J. Society of Naval Architects of Japan, Vol.158, pp.125-136 (in Japanese).
- [12] Yoshimura, Y. (1986): Mathematical Model for the Manoeuvring Ship Motion in Shallow Water, J. Kansai Society of Naval Architects, Japan, No.200, pp.41-51 (in Japanese).
- [13] Newman, J. N. (1977): Marine Hydrodynamics, The MIT Press, pp.132-140.
- [14] Newman, J. N. (1992): The Green Function for Potential Flow in a Rectangular Channel, J. Engineering Mathematics, 26, pp.51-59.
- [15] Yasukawa, H., Kawamura, S., Tanaka, S. and Sano, M. (2009): Evaluation of Ship-Bank and Ship-Ship Interaction Forces using a 3D Panel Method, Proc. Int. Conf. on Ship Manoeuvring in Shallow and Confined Water: Bank Effects, Antwerp, Belgium, pp.127-133.
- [16] Fujiwara, T., Ueno, M. and Nimura, T. (1998): Estimation of Wind Forces and Moments acting on Ships, J. Society of Naval Architects of Japan, Vol.183, pp.77-90. (in Japanese)

- [17] Spyrou, K. J., Tigkas, I. and Chatzis, A. (2007): Dynamics of a Ship Steering in Wind Revisited, *Journal of Ship Research*, Vol.51, No.2, pp.160-173.
- [18] Yasukawa, H., Hirono, T., Nakayama, Y. and Koh, K. K. (2012): Course Stability and Yaw Motion of a Ship in Steady Wind, *J. Marine Science and Technology*, Vol.17, No.3, pp.291-304.